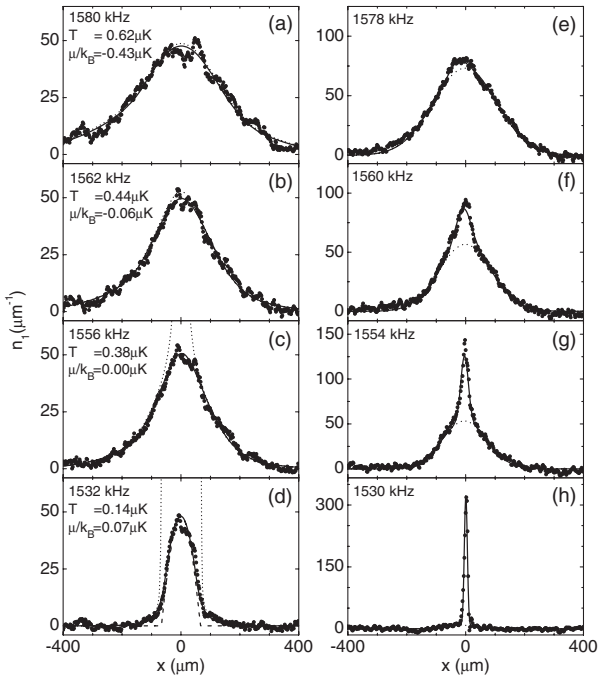

FIG. 1. Linear atomic density from absorption images obtained *in situ* (a)–(d) and *in focus* (e)–(h) by lowering (from top to bottom as indicated) the final rf evaporation frequency. *In situ*: solid lines are fits using Yang-Yang thermodynamic equations (see text). The values of μ and T resulting from the fits are shown in the figure. Dotted line: ideal Bose-gas profile showing divergence for $\mu(x) = 0$. Dashed line in (d): quasicondensate profile with the same peak density as the experimental data. *In focus*: solid lines are the sum of two independent Gaussian fits—one to the wings (dotted lines) and one to the central part of the density profile.

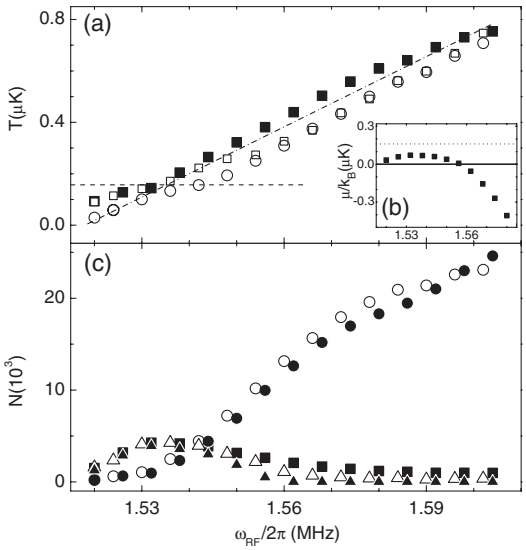

FIG. 2. Characterization of the atomic clouds as a function of the final rf frequency, as determined from fits of the Yang-Yang model to the *in situ* data and Gaussian fits to the *in focus* data. (a) Temperature from the *in situ* data (■) and from the radial (□) and axial (○) size of the broad Gaussian fit to the *in focus* data. The dash-dotted line is to guide the eye and indicates a ratio of 11 of the trap depth and the cloud temperature; dashed line corresponds to $\hbar\omega_\perp/k_B$. (b) Chemical potential from the Yang-Yang fit; dashed line indicates $\hbar\omega_\perp/k_B$. (c) Atom number from the *in focus* data: wide distribution (○) and central peak (△); from the Yang-Yang model fit to the *in situ* data: atoms in the radial ground state (■), in radially excited states (•), and atoms in the radial ground state experiencing $\mu(x) > 0$ (▲).

rium with the gas in the radial ground state, $\mu_j(x) = \mu(x) - j\hbar\omega_\perp$ [22]. Within this model, the linear density is given by

$$n_1(x, \mu, T) = n_{\mathrm{YY}}[\mu(x), T] + \sum_{j=1}^{\infty}(j+1)n_e[\mu_j(x), T].$$

For the radially excited states, we use the result of the LDA for the 1D ideal gas, $n_e(\mu_j, T) = g_{1/2}[\exp(\mu_j/k_BT)]/\Lambda_T$ where $g_{1/2}$ is a Bose function and $\Lambda_T = (2\pi\hbar^2/mk_BT)^{1/2}$ is the thermal de Broglie wavelength [1,15]. Note that as long as $\mu < \hbar\omega_\perp$, we have $\mu_j < 0$ which is necessary to avoid divergence of $g_{1/2}$. In this model, the radially excited states act as a bath for particle and energy exchange with the radial ground state. The resulting fits are shown as solid lines in Figs. 1(a)–1(d) and describe our data very well. The fitted values of T and μ are displayed in Fig. 2.

We now turn to the *in focus* measurements which give access to the axial momentum distribution of the gas. The focusing pulse is created by ramping up the axial trapping frequency from 8.5 to 20 Hz in 0.8 ms, maintaining this for 3.8 ms, and ramping back to 8.5 Hz in 0.8 ms, followed by a sudden switch-off of the magnetic trap. During the focusing pulse, the cloud length reduces by less than 20%. After switching off the magnetic trap, the cloud expands in the radial direction on a time scale of $1/\omega_\perp$ so that the interactions vanish rapidly compared to the relevant axial time scale, and the subsequent axial contraction can be treated as free propagation. After 13 ms of free propagation, the cloud comes to a focus.

In Figs. 1(e)–1(h), we show the axial density distribution obtained in the focus, averaged over typically 10 shots, for final rf frequencies similar to the *in situ* data in Figs. 1(a)–1(d). Here, in contrast to the *in situ* results, one can clearly distinguish a narrow peak from a broad pedestal for rf values below 1.56 MHz [Figs. 1(g) and 1(h)]. The Yang-Yang solution does not yield the momentum distribution, and thus it can not be used to fit to the *in focus* data. Instead, to quantify the observation of the bimodal structure, we first fit a 2D Gaussian to the wings of the atomic density distribution. In a second step, we fit a narrow Gaussian to the residual peak in the center. The fitted curves are shown after integration in the z direction in Figs. 1(e)–1(h), and describe the observed *in focus* distributions well. Figure 2(c) shows the resulting atom numbers in the wide and narrow part of the momentum distribution; we also plot the atom numbers from the Yang-Yang model in the radial ground state, in the radially excited states, and atoms in the radial ground state experiencing $\mu(x) > 0$. Comparing the *in situ* and the *in focus* data, we conclude